

See discussions, stats, and author profiles for this publication at: <https://www.researchgate.net/publication/262304762>

# Picosecond Pulse Radiolysis of Highly Concentrated Sulfuric Acid Solutions: Evidence for the Oxidation Reactivity of Radical Cation $\text{H}_2\text{O}(\cdot+)$

ARTICLE in THE JOURNAL OF PHYSICAL CHEMISTRY A · MAY 2014

Impact Factor: 2.69 · DOI: 10.1021/jp503861h · Source: PubMed

CITATIONS

4

READS

92

## 3 AUTHORS:



**Jun Ma**

Université Paris-Sud 11

15 PUBLICATIONS 79 CITATIONS

SEE PROFILE



**Uli Schmidhammer**

Université Paris-Sud 11

54 PUBLICATIONS 514 CITATIONS

SEE PROFILE



**Mehran Mostafavi**

Université Paris-Sud 11

162 PUBLICATIONS 2,902 CITATIONS

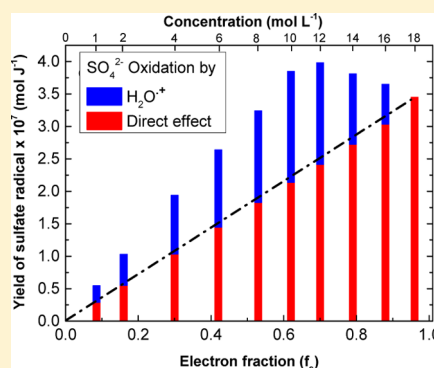
SEE PROFILE

# Picosecond Pulse Radiolysis of Highly Concentrated Sulfuric Acid Solutions: Evidence for the Oxidation Reactivity of Radical Cation $\text{H}_2\text{O}^{\bullet+}$

Jun Ma, Uli Schmidhammer, and Mehran Mostafavi\*

Laboratoire de Chimie Physique, CNRS/Université Paris-Sud, Bât. 349, 91405 Orsay, France

**ABSTRACT:** Aqueous solution of sulfuric acid is used as a suitable system to investigate the reactivity of the short-lived radical cation  $\text{H}_2\text{O}^{\bullet+}$  which is generated by radiation in water. Ten aqueous solutions containing sulfuric acid with concentration from 1 to 18 mol L<sup>-1</sup> are studied by picosecond pulse radiolysis. The absorbance of the secondary radical  $\text{SO}_4^{\bullet-}$  (or  $\text{HSO}_4^{\bullet-}$ ) formed within the 10 ps electron pulse is measured by a pulse–probe method in the visible range. The analysis of the kinetics show that the radicals of sulfuric acid are formed within the picosecond electron pulse via two parallel mechanisms: direct electron detachment by the electron pulse and oxidation by the radical cation of water  $\text{H}_2\text{O}^{\bullet+}$ . In highly concentrated solution when  $\text{SO}_4^{2-}$  is in contact with  $\text{H}_2\text{O}^{\bullet+}$ , the electron transfer becomes competitive against proton transfer with another water molecule. Therefore,  $\text{H}_2\text{O}^{\bullet+}$  may act as an extremely strong oxidant. The maximum radiolytic yield of scavenged  $\text{H}_2\text{O}^{\bullet+}$  is estimated to be  $5.3 \pm 0.1 \times 10^{-7} \text{ mol J}^{-1}$ .



## INTRODUCTION

Since the realization of nanosecond pulse radiolysis,<sup>1</sup> the study of the reactivity of radicals issued from water in diluted solutions has allowed obtaining a huge amount of rate constants and radical yields which are currently used in several fields of chemistry and biology.<sup>2</sup> In the case of concentrated solutions, the kinetics can be ultrafast and the mechanisms are more complex. Certain reactions can occur without any diffusion in solution on the time scale ranging from femtoseconds up to picoseconds. To study the radiation damage on materials and biosystems, there are two main reasons to consider picosecond pulse radiolysis measurements of concentrated aqueous solutions. First, the highly concentrated solutions are used in some applications where the ionizing radiation is present. For instance, in the uranium and plutonium separation process, concentrated nitric acid solutions are used and it is important to know how the yields and mechanisms of the radicals induced by radiation in such solutions are modified compared to those in dilute solutions. Second, the highly concentrated solutions could be used as models for studying interface systems which are not easy to study directly by pulse radiolysis. Two examples can be given: it is known that a large amount of water molecules are in direct contact with biomolecules such as DNA. When ionizing radiation is applied, a part of the radiation energy is absorbed directly by biomolecules, but a part is also absorbed by the water layer adjacent to biomolecules.<sup>3,4</sup> Therefore, the mechanism and the yield of the different contributions on the damage are complex and very difficult to understand if only the observations in dilute solution are the reference for such systems. Another example is the case of nuclear waste storage or the case when the heart of a nuclear power plant comes into

contact with water after an accident such as the one that occurred in Fukushima. In these cases, the amount of radiation dose deposited at the interface of radioactive material (nuclear waste or nuclear combustible) and water is very strong and the yields and the mechanisms of radicals produced at the interface could be very different than those in pure water or in diluted solutions. Recently, it was suggested that the interaction of the damaged cores of the Fukushima Daiichi nuclear reactors with cooling water could lead to the fast and unexpected dissolution of <sup>137</sup>Cs because of strong oxidizing radiation.<sup>5</sup> Against this background, it is necessary to develop approaches for understanding the mechanism induced at interfaces during radiation damage, and one of them is to study the radiolysis of concentrated solutions with picosecond pulse–probe methods.

The radiation effect on concentrated aqueous solutions was studied during the 1960s and 1990s.<sup>6</sup> The time-resolved measurements were limited to the microsecond and nanosecond range. The yields of the direct effect given in the published works were limited to these time windows, and the spur reactions of the radicals produced by direct effect were often ignored or not discussed. Moreover, the reactivity of short-lived radical cation  $\text{H}_2\text{O}^{\bullet+}$  was evoked without deducing a firm conclusion about its contribution on the oxidation mechanism of the solute. Picosecond pulse radiolysis is a great method allowing the measurement of the yields at ultrashort times when the spur reactions are still negligible. Several studies in highly concentrated  $\text{Br}^-$ ,  $\text{Cl}^-$ , and  $\text{HNO}_3$  solutions were undertaken.<sup>7–11</sup> Together with the theoretical

Received: April 20, 2014

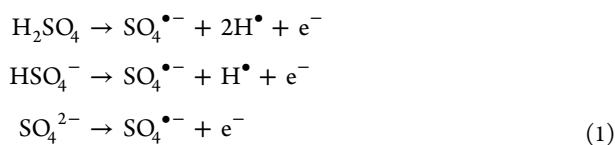
Revised: May 9, 2014

Published: May 13, 2014

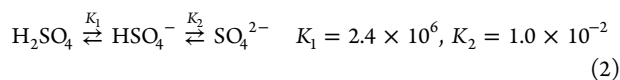
simulations, it was suggested that for highly concentrated solutions the proton-transfer reaction between  $\text{H}_2\text{O}^{\bullet+}$  and a water molecule becomes less efficient if the number of water molecules in close proximity of the radical cation decreases.

Radiolysis of sulfuric acid aqueous solutions has been extensively investigated over the past decades because it is commonly used in Fricke and Ceric sulfate dosimeters.<sup>12,13</sup> Several observations showed that the yields of the radicals and molecular products in aqueous solutions containing sulfuric acid strongly depend on the solute concentrations.<sup>14–16</sup> Early in the 1950s, it was postulated that the formation of  $\text{H}_2\text{S}_2\text{O}_8$  and  $\text{H}_2\text{SO}_5$  under irradiation provides the evidence that the radicals from water radiolysis interact with the sulfuric acid molecule.<sup>17</sup> The  $\text{OH}^\bullet$  radicals acting as the oxidizing intermediates were thought to attack the molecules  $\text{H}_2\text{SO}_4$  or its anions.<sup>18</sup> This view was further supported by determining the relative rate constant of the reaction between  $\text{OH}^\bullet$  radicals and sulfate anions in  $\text{Ce}^{\text{III}}$  salt systems.<sup>19</sup> In the beginning of the 1960s, yields of all the postulated intermediates in sulfuric acid solutions were established by Boyle over the concentration from 0.4 to 18 M.<sup>15,16</sup> It was pointed out that some of the primary excitations and ionizations are expected to occur in dissociated sulfuric molecules and ion species if the electron fraction is high enough. Although no direct proof was reported on the oxidizing radicals generated by water radiolysis attacking the solutes or the direct oxidizing of solutes, both of these processes were believed to be valid.<sup>16</sup> With the advent of the pulse radiolysis technique in the 1960s, the formation and yield measurement of sulfate radical ( $\text{SO}_4^{\bullet-}$  or  $\text{HSO}_4^\bullet$ ) became a central issue because it was identified as one of the major transients in radiolysis of sulfuric acid.<sup>20</sup> It was also shown that the yields of observed  $\text{SO}_4^{\bullet-}$  within a 12 ns electron pulse are linearly proportional with the electron fraction over the range from  $\sim 0.01$  to 0.3, giving clear evidence of  $\text{SO}_4^{\bullet-}$  formed by direct ionization of sulfuric acid anions.<sup>21</sup>

More recently, Katsumura et al. established a model stating that a fast formation process occurring within the 100 ns electron pulse is the direct radiolytic effect on the solutes according to the following reactions:<sup>22</sup>

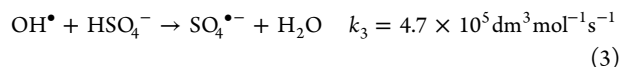


Sulfuric acid is a strong diprotic acid and dissociates when dissolved in water described by following equilibria:



The concentration of each species changes as the total concentration changes, but  $\text{HSO}_4^-$  anion is observed over the entire concentration.

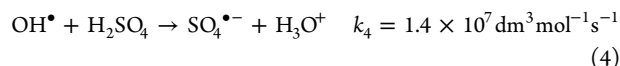
When diluted solutions of sulfuric acid are irradiated, the H-abstraction reaction takes place between  $\text{HSO}_4^-$  anion and  $\text{OH}^\bullet$  radical, forming the sulfate radical



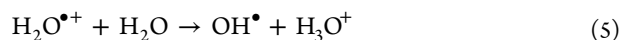
In radiolysis of a neutral lithium sulfate aqueous solution, the additional sulfate radical formation is not observed in the kinetics apart from the contribution of fast direct action of

radiation. Consequently, it was concluded that  $\text{OH}^\bullet$  is not likely to react with sulfate anions  $\text{SO}_4^{2-}$ .<sup>22</sup>

As the acid aqueous solution becomes concentrated, the amount of undissociated sulfuric acid is not negligible and the sulfuric acid participates in reacting with  $\text{OH}^\bullet$ :



The possibility of electron transfer from solutes to the primary positive holes  $\text{H}_2\text{O}^{\bullet+}$  in aqueous systems as another mechanism was also evoked without a consistent conclusion. In neat water, the proton-transfer reaction occurs on ultrafast time scale ( $< 100$  fs) as the surrounding water responds to the trapping hole very quickly:



Therefore, three distinct processes are discussed to be involved in the formation mechanism of sulfate radical: (i) reaction of  $\text{OH}^\bullet$  with hydrogensulfate anions ( $\text{HSO}_4^-$ ) and undissociated  $\text{H}_2\text{SO}_4$ ,<sup>19,20,22,23</sup> (ii) direct action of ionizing radiation on solutes in sulfuric acid,<sup>23,22,24</sup> (iii) reaction of sulfuric acid with the positive radical ion  $\text{H}_2\text{O}^{\bullet+}$ , the precursor of the  $\text{OH}^\bullet$  radical.<sup>12,25</sup>

It may be pointed out that highly concentrated (multimolar) sulfuric acid solutions are an appropriated model system to elucidate the occurrence of the different mechanisms by picosecond pulse radiolysis. The study of sulfuric acid solutions can be motivated by several reasons: (i) several simulations of water/ $\text{H}_2\text{SO}_4$  mixtures are reported showing that the separation in two phases by clustering does not occur in these solutions.<sup>26,27</sup> Therefore, these solutions can be considered as a homogeneous system even at high concentrations. This point is important because if a nonhomogenous distribution of water molecules takes place, the treatment of the kinetics becomes nontrivial. (ii) In contrast to the halides and nitric acid solutions, as the rate constant of the reactions of solutes in sulfuric acid solution with  $\text{OH}^\bullet$  is rather low, these reactions are unlikely in the picosecond time scale even at very high concentration. In fact, if the oxidation reaction by  $\text{OH}^\bullet$  radical occurs at short times, it becomes very difficult to distinguish between  $\text{OH}^\bullet$  and its precursor contribution on the oxidation mechanism. (iii) Usually the following relation is used for the experimental yield:

$$G_{\text{exp}} = f_s G_{\text{dir}} + f_w G_{\text{indir}} \quad (6)$$

where  $G_{\text{dir}}$  is the yield of direct ionization of solutes and  $f_w$  is the fraction of water electron density. The yield of reaction produced by the water radical is denoted  $G_{\text{indir}}$ . In the case of sulfuric acid solutions, the following relationship between the electron fractions and the molar ratio of solvent and solutes can be considered:

$$f_s = 1 - f_w = \frac{50 \times [\text{SO}_4^{2-}]}{10 \times [\text{H}_2\text{O}] + 50 \times [\text{SO}_4^{2-}]} \quad (7)$$

$\text{SO}_4^{2-}$  represents the sulfur compounds including the anions and the undissociated molecule. In the case of sulfuric acid solutions, it is possible to investigate almost neat liquid sulfuric acid, thus eliminating the contribution of water radiolysis. Therefore, the radiolytic yield of the oxidation via the direct effect of radiation on this solution can be obtained ( $f_s$  almost 1). This important point was missing with NaBr, NaCl, and  $\text{HNO}_3$  solutions because of the lower solubility at room

temperature. In fact, the direct access to the yield of direct effect at the picosecond range is decisive. (iv) Sulfuric acid is a strong acid and insensitive to proton transfer. (v) The uncertainty of the radical yield depends on the uncertainty of the extinction coefficient of the secondary radical; in the case of sulfuric acid, the molar absorption coefficient of  $\text{SO}_4^{\bullet-}$  is well-established by different radiolysis<sup>22,21</sup> or photolysis<sup>28,29</sup> methods and can be used for the precise determination of the radiolytic yield. (vi) Contrary to the metal cation such as  $\text{Na}^+$ , the counterions  $\text{H}^+$  are not involved in the direct effect. This point is also very important because the metal cations could lose their electron by direct effect and render, even if this process is transient, the further electron-transfer mechanism more complex. (vii) The reduction potential of the couple  $\text{SO}_4^{\bullet-}/\text{SO}_4^{2-}$  is well-known to be as high as 2.5  $V_{\text{NHE}}$ . If a chemical species can oxidize  $\text{SO}_4^{2-}$  (or  $\text{HSO}_4^-$ ), its reduction potential can be considered to be higher.

For the above seven reasons,  $\text{H}_2\text{SO}_4/\text{H}_2\text{O}$  constitutes a suitable model system to study the direct effect of ionizing radiation and to show the possible oxidizing reactivity of  $\text{H}_2\text{O}^{\bullet+}$ . In our recent publication, it was shown that the radical cation contributes to the oxidation mechanism.<sup>30</sup> In the present work on concentrated sulfuric acid solutions, additional experimental results and their full analysis are presented. Ten solutions containing sulfuric acid from 1 to 18  $\text{mol L}^{-1}$  are studied by picosecond pulse radiolysis, particularly by measuring the absorbance of the secondary radical  $\text{SO}_4^{\bullet-}$  (or  $\text{HSO}_4^{\bullet}$ ) formed within the electron pulse.

## EXPERIMENTAL SECTION

The transient absorption pulse–probe setup is based on the laser–electron intrinsic synchronization resulting from the laser-triggered photocathode and was detailed elsewhere.<sup>31</sup> Briefly, the main part of a femtosecond Ti:sapphire laser output is frequency tripled and used to produce the electron pulse that is accelerated by the radio frequency fields. A part of the laser source is split off to generate the optical probe pulse that can be delayed relative to the electron bunch by a mechanical translation stage.

As described in ref 32, multiple probe wavelengths can be generated and recorded synchronously by a multichannel detection system placed in the focal plane of a polychromator. The kinetics of several transient species absorbing at different wavelengths in the ultraviolet (UV) to visible can be recorded under identical experimental conditions. Here we used the option of the supercontinuum generated in  $\text{CaF}_2$  as probe light to acquire entire visible transient spectra independently of the shot-to-shot fluctuations and possible long-term drifts of the electron source operated at 10 Hz. A reference signal is split off from the broadband probe before the fused silica optical flow cell (FSOFC). Probe and reference beams were each coupled into an optical fiber, transmitted to a spectrometer, and dispersed onto a charge-coupled device.

All the measurements were made in a FSOFC with a 5 mm optical path in solution that is collinear to the electron pulse propagation. The electron pulses had a charge of about 4 nC and a duration <10 ps; the electron energy was 6–8 MeV. Under these conditions, the time resolution is mainly determined by the electron pulse duration and the velocity mismatch between the electron pulse and the slower visible probe pulse during their propagation inside the cell. Fitting the rise of the absorption signal of the solvated electron, a species that is formed on the femtosecond scale, by a step function

convoluted with a Gaussian cross-correlation revealed an apparatus function of full width at half-maximum of 12 ps. More details on the optical configuration and the data acquisition can be found in ref 32. The cited publication also reveals and quantifies transient absorption induced by the electron pulse in the windows of an empty FSOFC. In the present work we used a new, custom-made FSOFC that reduces the thickness of the entrance and exit window at the intersection with the probe beam by a factor of 5, to 200  $\mu\text{m}$  (Figure 1). In consequence and as discussed in ref 32, the

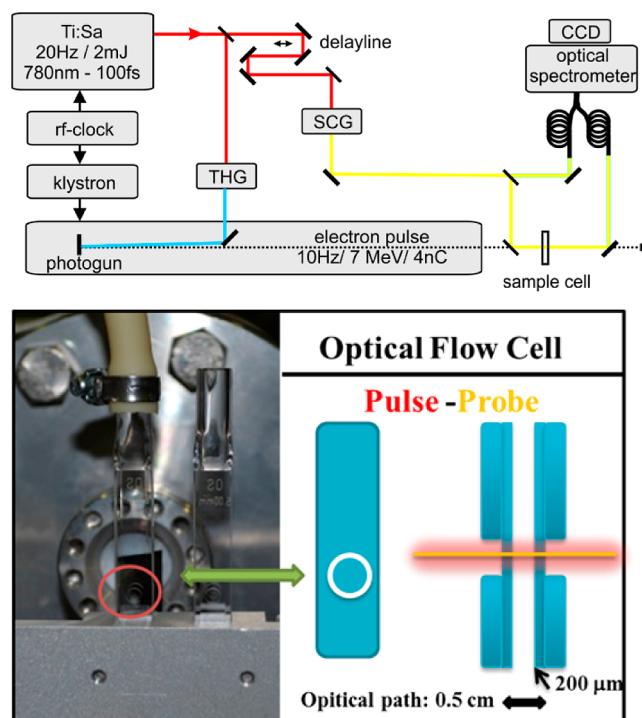


**Figure 1.** Scheme of the electron pulse–broadband probe setup and the fused silica optical flow cell (FSOFC). Two identical optical cells placed on a translation stage system are used as shown in photo; the right cell contains neat water to measure the dose per pulse for each experiment; the kinetics of the solutions under study are recorded in the left cell. At the intersection with pump and probe beams, the thickness of the walls of the cell windows is only 200  $\mu\text{m}$ .

absorbance induced by the electron pulse in the cell is 5 times less than that measured previously. In our configuration in the visible range, the absorbance in the empty cell just after the pulse is less than 1.1 mOD (value at maximum of the absorption around 600 nm) for an absorbed dose of 31.3  $\text{J kg}^{-1}$  per pulse.

After the remaining contribution of the cell windows is subtracted, the transient absorption in pure water measured in the visible and near-infrared is due to the hydrated electron; this is used as reference for dosimetry on the basis of  $G_{e_s^-} = 4.25 \times 10^{-7} \text{ mol J}^{-1}$  at 10 ps.<sup>33</sup> The energy deposited in concentrated solutions  $D_{\text{sol}}$  is increased relative to neat water by the direct radiation effect on the solute molecules. The effective dose considering this contribution can be derived from the reference dose in pure water  $D_w$  as follows:

$$D_{\text{sol}} (\text{J L}^{-1}) = F D_{\text{water}} (\text{J kg}^{-1}) \quad (8)$$

with



**Table 1.** Concentration of Sulfuric Acid Solutions and Their Corresponding Parameters: Electron Density Fraction of Solute  $f_s$ , Electron Density Fraction of Water  $f_w$ , Dose Factor  $F$ , and Solution Density  $d_{\text{sol}}^a$ 

C (mol L <sup>-1</sup> )	$f_s$	$f_w$	$F$ (g cm <sup>-3</sup> )	$d_{\text{sol}}$ (g cm <sup>-3</sup> )	$[\text{H}_2\text{O}]/[\text{H}_2\text{SO}_4]$	$A_{\text{SO}_4^{\bullet-}} (\times 10^3) (t = 15 \text{ ps})$	$G_{\text{SO}_4^{\bullet-} 15 \text{ ps}} (\times 10^7 \text{ mol J}^{-1})$
1	0.085	0.915	1.05	1.06	53.6	1.38	0.55
2	0.16	0.84	1.11	1.12	25.7	2.58	1.03
4	0.30	0.70	1.20	1.23	11.7	4.87	1.94
6	0.42	0.58	1.29	1.34	7.0	6.59	2.64
8	0.53	0.47	1.38	1.44	4.58	8.12	3.24
10	0.62	0.38	1.46	1.54	3.10	9.64	3.85
12	0.70	0.30	1.55	1.65	2.06	10.01	3.98
14	0.79	0.21	1.64	1.74	1.33	9.55	3.81
16	0.88	0.12	1.67	1.80	0.68	9.14	3.65
18	0.96	0.04	1.69	1.83	0.23	8.64	3.45

<sup>a</sup>The absorbance of  $\text{SO}_4^{\bullet-}$  at 10 ps is deduced by  $A_{\text{SO}_4^{\bullet-}}(t = 15 \text{ ps}, \lambda = 450\text{--}460 \text{ nm}) = A_{\text{obs}}(t = 15 \text{ ps}, \lambda = 450\text{--}460 \text{ nm}) - A_{\text{solvated electron}}(t = 15 \text{ ps}, \lambda = 450\text{--}460 \text{ nm}) - A_{\text{FSOFC}}(t = 15 \text{ ps}, \lambda = 450\text{--}460 \text{ nm})$ . The value of the absorbance due to the transient induced in the walls of FSOFC around 450 nm,  $A_{\text{FSOFC}}(15 \text{ ps})$ , is  $6.34 \times 10^{-4}$  based on the work reported in ref 32.

$$F = d_{\text{sol}} [Z_{\text{SO}_4^{2-}} p / A_{\text{H}_2\text{SO}_4} + Z_{\text{water}} (100 - p) / A_{\text{water}}] (Z_{\text{water}} 100 / A_{\text{water}})^{-1} \quad (9)$$

Where  $d_{\text{sol}}$  is the density of the solution,  $Z$  the number of electrons,  $A$  the mass number, and  $p$  the percentage of weight fraction of the solute. The value of  $F$  and other physicochemical properties for the investigated sulfuric acid aqueous solutions from 1 to 18 M are summarized in Table 1.

The solutions containing sulfuric acid at high concentration and neat water were studied under identical experimental conditions. Particular attention was paid for a constant dose. Two identical FSOFC, one for the solutions and one for neat water, were placed side-by-side on a translation stage (Figure 1). This allows rapid switching between solution and dosimetry measurements; the dose was measured before each experiment series and checked during it. Transient spectra were recorded on the picosecond scale; the kinetics were traced after data acquisition at selected wavelengths. The temporal evolution of each sample under investigation was scanned on the order of 30 times with a single-point averaging of 10 for each delay step. The measurements were performed at 22.5 °C, the room temperature during the picosecond pulse radiolysis experiments. The sulfuric acid was purchased from Sigma-Aldrich. Water for dilution was purified by passage through a Millipore purification system.

## RESULTS AND DISCUSSION

The transient absorption spectra for different solutions (1–18 M sulfuric acid) recorded around 15 ps are shown in Figure 2.

For concentrations of 1–4 M, the spectra show the contribution of solvated electron with its typical large absorption centered in the red; for the solutions containing higher concentrations, an absorption band with a maximum around 450 nm becomes evident. The kinetics traced at 450 and 730 nm are shown in Figure 3 for each solution and for the same absorbed dose, i.e., after correction with the factor  $F$ . At 730 nm, the slow decay observed for pure water is accelerated by increasing the acid concentration. In the case of lower concentrations, a fast decay is observed at short time (the half time decay is 50, 25, and 10 ps for 1, 2, and 4 M, respectively). As the concentration is further increased, the decay becomes too fast to be resolved; the solvated electron is completely scavenged within the electron pulse for solutions at concentration higher than 6 M. It can be noted that also the

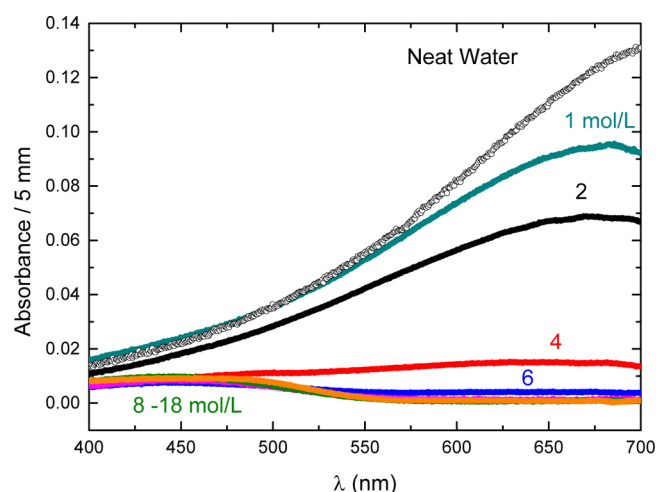
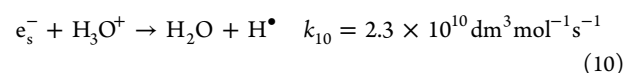


**Figure 2.** Transient absorption spectra recorded directly after the picosecond electron pulse (15 ps after time zero) in 1–18 M  $\text{H}_2\text{SO}_4$ . The contribution of transient absorption induced in the FSOFC windows is subtracted. The radiation dose deposited in neat water is 31.3 Gy.

initial absorbance amplitude at 730 nm due to the solvated electron is decreased by increasing the acid concentration from neat water solution to 4 M sulfuric acid solution. The kinetics at 450 nm are very different from those observed at 730 nm. For lower concentrations (1, 2, and 4 M), a fast decay as at 730 nm is observed but the decay is never total and reaches a plateau. For higher concentration, the kinetics at 450 nm is very slow. The amplitude of the absorbance increases with increasing acid concentration up to 12 M, and then it decreases for the highest concentration (14, 16, and 18 M). The decay observed at 450 nm is due to the spur reactions, mainly with  $\text{H}^\bullet$  atom similar to the reactions reported for  $\text{OH}^\bullet$  radical in water.<sup>34</sup>

In highly acidic solution, the decay of solvated electron (at 730 nm, Figure 3) is attributed mainly to the following reaction:



$\text{H}^\bullet$  effectively reacts with the solvated electron and produces radical  $\text{H}^\bullet$  in the spurs. The  $\text{H}^\bullet$  atom absorbs far in the UV. Moreover, it is important to note that the presolvated electron is also scavenged by  $\text{H}^\bullet$ . This is why the initial absorbance

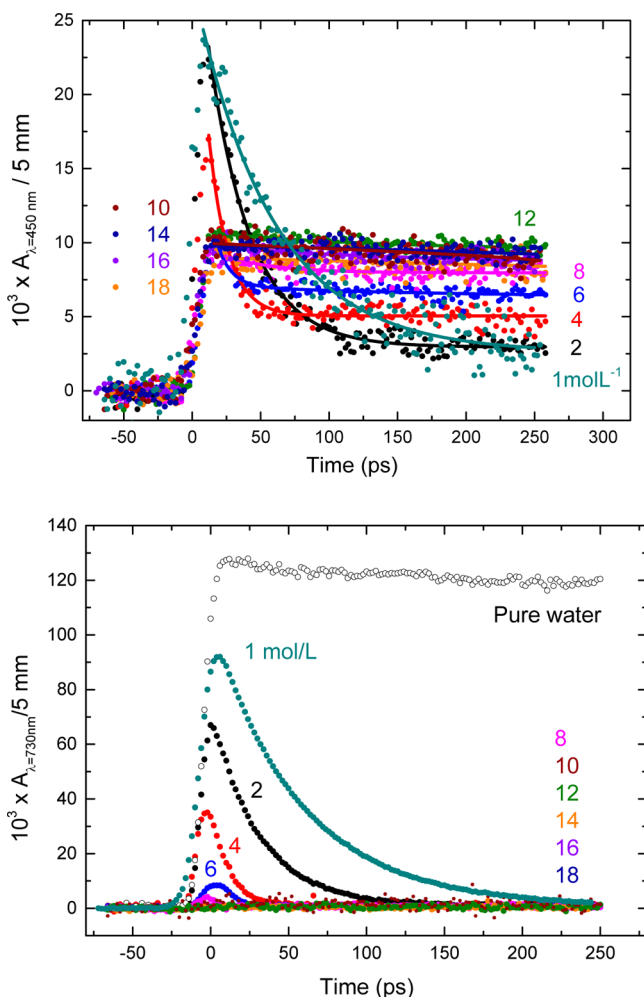


**Figure 3.** (a) Kinetics at 450 nm on the picosecond scale for solutions containing  $\text{H}_2\text{SO}_4$  with different concentrations. (b) Kinetics at 730 nm for pure water and solutions containing  $\text{H}_2\text{SO}_4$  with different concentrations. In panels a and b, the transient absorbance amplitude was corrected by the factor  $F$  to consider the density effect (see text).

around 730 nm is decreased by increasing the concentration of acid. This decrease of the initial absorbance is also partly due to the shift of the absorption band of solvated electron which is dependent on the concentration of sulfuric acid. Under our experiment conditions, the pulse–probe absorption measurements contain not only the contribution of  $\text{SO}_4^{\bullet-}$  (or  $\text{HSO}_4^{\bullet-}$ ) but also that of transient species induced in FSOFC as well as that of nonscavenged solvated electron in the case of less concentrated sulfuric acid solutions. The absorption spectra obtained after subtraction of the contributions of the transients induced in FSOFC and of the solvated electron are reported in Figure 4. An absorption band is clearly observed around 450 nm, which is in excellent agreement with the literature values of the typical spectra of  $\text{SO}_4^{\bullet-}$  produced by radiolysis<sup>22,21</sup> or photolysis<sup>28,29</sup> both in diluted and concentrated solutions up to 10 M.

The kinetics at 450 and 730 nm are selected for studying the reactions involving  $\text{SO}_4^{\bullet-}$  in concentrated solutions. To elucidate the detailed formation process of  $\text{SO}_4^{\bullet-}$ , the contribution of solvated electron is subtracted from kinetics presented in Figure 3. Figures 4 and 5 show the kinetics of  $\text{SO}_4^{\bullet-}$  and its initial optical density, respectively.

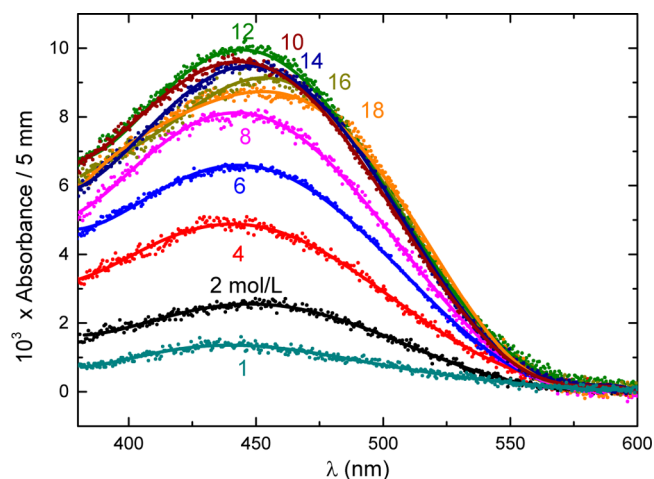


**Figure 4.** Transient absorption spectra of the radical ( $\text{HSO}_4^{\bullet}$  and  $\text{SO}_4^{\bullet-}$ ) recorded at 15 ps in 1–18 M  $\text{H}_2\text{SO}_4$ . The contribution of solvated electron in 1–6 M  $\text{H}_2\text{SO}_4$  is subtracted from the signal.

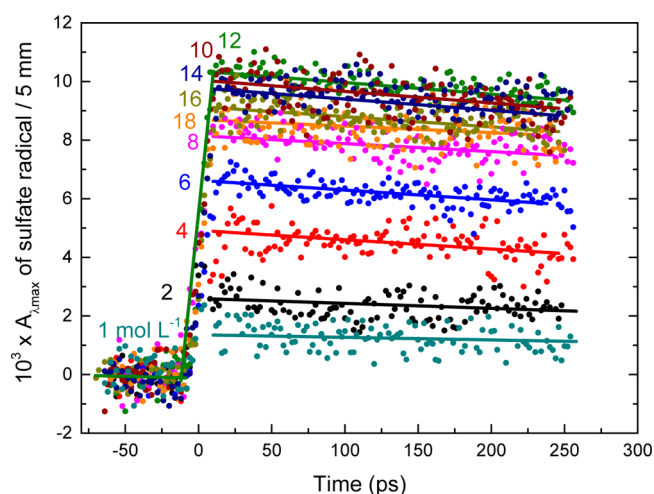


**Figure 5.** Kinetics of radical ( $\text{HSO}_4^{\bullet}$  traced at 460 nm or  $\text{SO}_4^{\bullet-}$  traced at 450 nm) in 1–18 M  $\text{H}_2\text{SO}_4$ . The contribution of solvated electron in 1–6 M  $\text{H}_2\text{SO}_4$  is subtracted from the signal.

If for the formation of the radical of sulfuric acid only the direct radiolytic effect is considered, the optical density of radical  $\text{SO}_4^{\bullet-}$  is supposed to be proportional to the electron fraction of solutes  $f_s$  at the same radiation dose.

Interestingly, the initial absorbance at 15 ps of  $\text{SO}_4^{\bullet-}$  increases in the first series of solutions as expected, but it reaches a maximum value at 12 M and then drops down slightly (Figure 6). This points out that a second parallel mechanism must be involved in the generation of the sulfate radicals. To obtain the yields of  $\text{SO}_4^{\bullet-}$  on the basis of the optical measurements in our experiment, the molar absorption coefficient  $\epsilon$  ( $\text{SO}_4^{\bullet-}$ , 450 nm) = 1600  $\text{dm}^3 \text{mol}^{-1} \text{cm}^{-1}$ , which has no significant change in the concentration range, is considered.

Assuming that  $\epsilon$  ( $\text{SO}_4^{\bullet-}$ , 450 nm,  $\text{HSO}_4^{\bullet-}$  460 nm) remains unchanged from 1 to 18 M, the experimental yield of  $\text{SO}_4^{\bullet-}$  (and  $\text{HSO}_4^{\bullet-}$ ) is calculated and presented in Table 1 and Figure 7. When the concentration of sulfuric acid is 18 M, the amount of water molecule is very rare and unlikely to produce the  $\text{H}_2\text{O}^{\bullet+}$ . Thus, the experimental yield  $G_{\text{exp}}$  value obtained for 18 M is considered to be almost the radiolytic yield of the

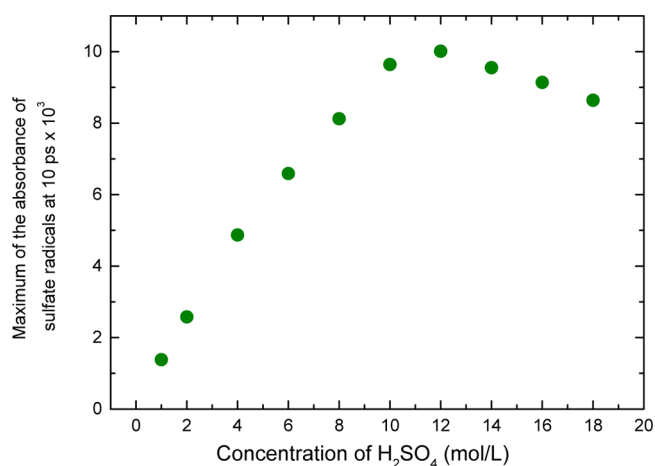


**Figure 6.** Amplitude of the absorbance at the maximum of band absorption recorded at 15 ps versus sulfuric acid concentration.

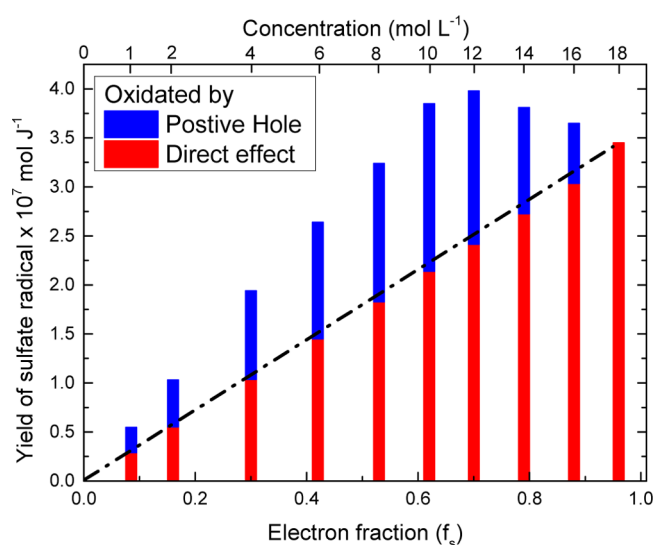
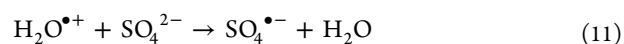


**Figure 7.** Yield of sulfuric acid radical formation versus electron fraction of the solute. The value at 18 M is considered to be the direct effect yield and is linearly extrapolated to the zero concentration. The supplementary yield is considered to be due to the electron-transfer reaction with radical cation  $\text{H}_2\text{O}^{\bullet+}$ .

direct effect ( $G_{\text{dir}} = 3.5 \pm 0.1 \times 10^{-7} \text{ mol J}^{-1}$ ). With this value and the zero point, the linear slope is plotted in Figure 7, denoting the contribution of the direct effect on the oxidation. This line shows clearly that the direct effect alone cannot be responsible for the ultrafast buildup of the oxidation products of sulfuric acid. For instance, in the case of 1 M sulfuric acid solution ( $f_s = 0.085$ ), if we consider only the direct effect for its formation, the value of direct effect yield must be  $6.5 \times 10^{-7} \text{ mol J}^{-1}$ , which is too large compared to the values usually reported for the direct effect yield (lower than  $5 \times 10^{-7} \text{ mol J}^{-1}$ ). Therefore, the observed yield cannot be explained by only the direct effect.

As the rate constant of  $\text{OH}^\bullet$  radical with solutes is low and the reaction is unlikely at the picosecond range, the only reaction that can explain the additional formation of this radical is due to the following reaction.



This contribution is not linear with the electron fraction and reaches its maximum for  $f_s = 0.6$ – $0.7$  (Figure 7). In fact, for the lowest concentrations (1 and 2 M) the amount of water is important and the radical cation  $\text{H}_2\text{O}^{\bullet+}$  reacts also with water molecule to form  $\text{OH}^\bullet$  radical. For the highest concentrated solutions, the amount of water is negligible and then the contribution of the proton-transfer reaction 5 is nonsignificant. From the data of Figure 7, the yield of radical cation  $\text{H}_2\text{O}^{\bullet+}$  scavenged by sulfuric acid is reported. It is interesting to note that the yield increases with the concentration of sulfuric acid and reaches a plateau with value around  $5.3 \times 10^{-7}$  (Figure 8).

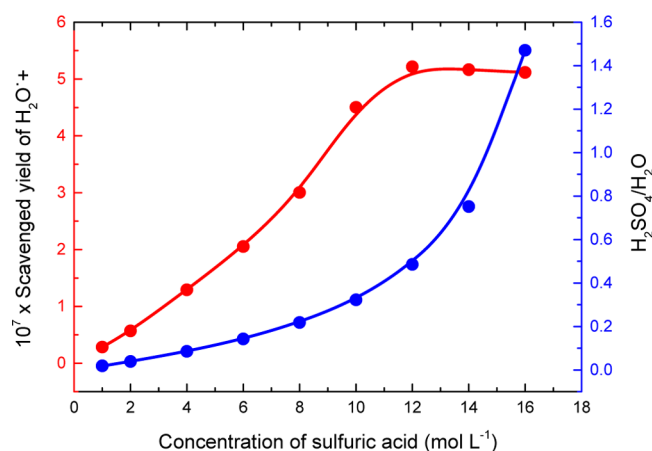


**Figure 8.** Yield ( $\text{mol J}^{-1}$ ) of scavenged radical cation  $\text{H}_2\text{O}^{\bullet+}$  obtained from the equation  $G_{\text{scv}} = (G_{\text{exp}} - f_s G_{\text{dir}})/(f_w)$  (left axis) and the ratio of  $\text{H}_2\text{SO}_4$  and water (right axis) as a function of sulfuric acid concentration in the aqueous solution.

Especially interesting is the behavior observed at concentrations of 12, 14, and 16  $\text{mol L}^{-1}$ , at which the amount of water is so low that reaction 5 is almost suppressed and  $\text{H}_2\text{O}^{\bullet+}$  scavenging occurs within a few tens of femtoseconds. For these three solutions, the yield of scavenged  $\text{H}_2\text{O}^{\bullet+}$  is found to be about  $(5.3 \pm 0.1) \times 10^{-7} \text{ mol J}^{-1}$ , which is larger than the yield of hydrated electron at 1 ps ( $4.7 \times 10^{-7} \text{ mol J}^{-1}$ ).<sup>35</sup> This means that reactions 5 and 11 are also in competition with the following geminate recombination:



Therefore, it can be considered that the yield of ionized water in the femtosecond range is no less than  $5.3 \times 10^{-7} \text{ mol J}^{-1}$ , within the experimental uncertainty.

Finally, the picosecond experimental yield of sulfuric acid radical formation plotted as a function of electron fraction is compared with the data given in the literature based on nanosecond pulse radiolysis (Figure 9). Obviously there is a strong dependence of the observed yield on the accessible time scale. To be best comparable with our condition, we report only the fast component of sulfuric acid radical yield, which is formed within the nanosecond pulses (duration 12 or 100 ns). In that case, a possible contribution of  $\text{OH}^\bullet$  radical is excluded. The experimental yield achieved by picosecond pulse radiolysis is distinctly higher than those obtained with nanosecond resolution. The data from Boyle are given over a large concentration range as in our work. His results obtained by using the scavenging method at 100 ns are also lower than those measured in this work because of the spur reactions of the secondary radical. But it is interesting that the same trend, a

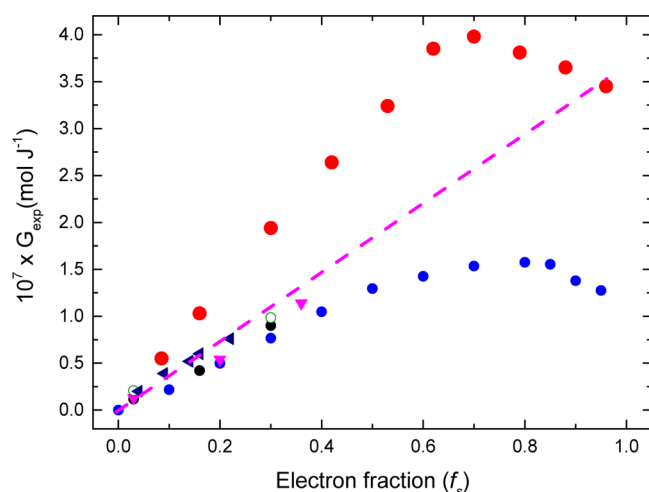


**Figure 9.** Experimental yield of sulfuric acid radical formation determined on different time scales versus electron fraction of the solute. For the studies using nanosecond pulses, only the yield of formation within the 10 or 100 ns electron pulse is reported in the literature; we corrected these data for comparison by using the same extinction coefficient  $\epsilon_{\lambda=450\text{ nm}} = 1600\text{ mol}^{-1}\text{ L cm}^{-1}$ . (Red circles) This work, within 10 ps pulse; (black circles) Lesign et al.<sup>21</sup> within 12 ns pulse; (blue circles) Boyle<sup>15</sup> scavenging at 100 ns; (red triangles) Katsumura et al. within 100 ns pulse;<sup>22</sup> (open circles) Sworski et al. 100 ns pulse;<sup>19</sup> (dark blue triangles) Katsumura et al. 100 ns pulse using  $\text{LiSO}_4$  solutions instead of  $\text{H}_2\text{SO}_4$ .<sup>22</sup> Dashed line is expressed to show the direct effect yield estimated in this work.

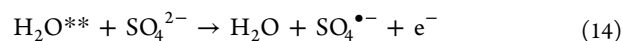
decrease of the yield at highest concentrations, was also observed by Boyle.<sup>15,16</sup>

By considering the competition reactions of the radical cation (reactions 5 and 11) a general equation allowing for the contributions of direct and indirect effect could be expressed as

$$G_{\text{exp}} = f_s G_{\text{dir}} + f_w G_{\text{indir}} \left( 1 + \frac{k_s [\text{H}_2\text{O}]}{k_{11} [\text{SO}_4^{2-}]} \right)^{-1} \quad (13)$$

But the fit of our data (Figure 9) by using Bayesian method show that such an equation cannot reproduce the experimental data with suitable and meaningful parameters for the yields. That means the use of rate constants is not valid for these reactions whatever the concentration. This point is understandable if we consider that the rate of hydrogen bonding, which is involved in the proton-transfer reaction in water solution (reaction 5), is drastically changed when the sulfuric acid concentration is increased. In fact, the presence of sulfuric acid changes the hydrogen bond net in water, and this change does not depend linearly on the water concentration.

At the end, the role of excited states is discussed in these processes. In fact, a part of the energy is absorbed by forming excited states. It is known that the yield of  $\text{H}_2\text{O}^{*+}$  channel forming  $\cdot\text{O}\cdot$ ,  $\text{H}\cdot$ , and  $\text{OH}\cdot$  is lower than that of ionization in neat water. Nevertheless, the amount of solvated electrons was also measured, and it is found that this amount (after correction with the factor  $F$ ) is not increased by increasing the solute concentration. Consequently, the channel involving the following reaction is not significant in our system:



Moreover, the excited state of  $\text{SO}_4^{2-*}$  could also be formed by electron pulse. These states can relax to the ground states,

form new radicals, or autoionize into the secondary radical  $\text{SO}_4^{\cdot-}$ . We considered this process as direct effect even if an ultrashort-lived transient excited state can be involved for the formation of  $\text{SO}_4^{\cdot-}$ .

## CONCLUSION

The pulse–probe measurements reported in this work show clearly that the radical of sulfuric acid can be formed via two mechanisms: direct electron detachment by the electron pulse and oxidation by the radical cation of water  $\text{H}_2\text{O}^{*+}$ . This latter has a very short lifetime in neat water, i.e., less than 100 fs. But in highly concentrated solution when another molecule is in contact with  $\text{H}_2\text{O}^{*+}$ , the electron transfer becomes competitive against proton transfer with another water molecule. Though often discussed in the past, the role of  $\text{H}_2\text{O}^{*+}$  in oxidation processes of irradiated systems was mostly a subject of controversy and speculation. Here, it has been clearly and quantitatively demonstrated by the picosecond pulse radiolysis of highly concentrated sulfuric acid that  $\text{H}_2\text{O}^{*+}$  may act as an extremely strong oxidant. Moreover, the radiolytic yield of  $\text{H}_2\text{O}^{*+}$  is found to be  $5.3 \pm 0.1 \times 10^{-7}\text{ mol J}^{-1}$ . This value is reasonable and is higher than the radiolytic yield of solvated electron published at very short times (1 ps). In fact, within the first picosecond, geminate recombination between presolvated electron and radical cation  $\text{H}_2\text{O}^{*+}$  occurs and reduces the yield of solvated electrons. In addition to irradiation of concentrated solutions of strong or even weak electron donors, the direct oxidation phenomenon by  $\text{H}_2\text{O}^{*+}$  can actually take place anywhere where the probabilities of its nearest neighbors being  $\text{H}_2\text{O}$  or another molecule are comparable. That is the case in all irradiated interfaces when irradiated water molecules are in contact with other molecules. Up to now, in the oxidation mechanism, only  $\text{OH}\cdot$  and  $\text{H}_2\text{O}_2$  are evoked, but our results show that even if  $\text{H}_2\text{O}^{*+}$  is short-lived, its involvement in oxidation mechanisms should be considered.

## AUTHOR INFORMATION

### Corresponding Author

\*E-mail: mehnan.mostafavi@u-psud.fr.

### Notes

The authors declare no competing financial interest.

## ACKNOWLEDGMENTS

The authors thank Pascal Pernot for helpful discussions and Alexandre Demarque for help during the realization of the new optical flow cell.

## REFERENCES

- (1) Hart, E. J.; Boag, J. W. Absorption Spectrum of the Hydrated Electron in Water and in Aqueous Solutions. *J. Am. Chem. Soc.* **1962**, *84*, 4090–4095.
- (2) Mallard, W. G.; Ross, A. B.; Helman, W. P. NDRL-NIST Solution Kinetics Database: Ver3. Notre Dame Radiation Laboratory and National Institute of Standards and Technology: Notre Dame, IN and Gaithersburg, MD, 1998.
- (3) O'Neill, P.; Stevens, D. L.; Garman, E. F. Physical and Chemical Consideration of Damage Induced in Protein Crystals by Synchrotron Radiation: A Radiation Chemical Perspective. *J. Synchrotron Radiat.* **2002**, *9*, 329–332.
- (4) Purkayastha, S.; Milligan, J. R.; Bernhard, W. A. Correlation of Free Radical Yields with Strand Break Yields Produced in Plasmid DNA by the Direct Effect of Ionizing Radiation. *J. Phys. Chem. B* **2005**, *109*, 16967–16973.



- (5) Grolmbow, B.; Mostafavi, M. State of Fukushima Nuclear Fuel Debris Tracked by Cs137 in Cooling Water. *Environ. Sci.: Processes Impacts*, submitted for publication 2014.
- (6) Katsumura, Y. Radiation Chemistry of Concentrated Inorganic Aqueous Solution. In *Radiation Chemistry Present Status and Future Trends*; Jonah, C. D., Rao, B. S. M., Eds.; Elsevier Science B.V.: Paris, 2001.
- (7) Balcerzyk, A.; Schmidhammer, U.; El Omar, A. K.; Jeunesse, P.; Larbre, J. P.; Mostafavi, M. Direct and Indirect Radiolytic Effects in Highly Concentrated Aqueous Solutions of Bromide. *J. Phys. Chem. A* **2011**, *115*, 4326–4333.
- (8) El Omar, A. K.; Schmidhammer, U.; Rousseau, B.; LaVerne, J.; Mostafavi, M. Competition Reactions of  $\text{H}_2\text{O}^+$  Radical in Concentrated  $\text{Cl}^-$  Aqueous Solutions: Picosecond Pulse Radiolysis Study. *J. Phys. Chem. A* **2012**, *116*, 11509–11518.
- (9) Balcerzyk, A.; LaVerne, J.; Mostafavi, M. Picosecond Pulse Radiolysis of Direct and Indirect Radiolytic Effects in Highly Concentrated Halide Aqueous Solutions. *J. Phys. Chem. A* **2011**, *115*, 9151–9159.
- (10) Balcerzyk, A.; El Omar, A. K.; Schmidhammer, U.; Pernot, P.; Mostafavi, M. Picosecond Pulse Radiolysis Study of Highly Concentrated Nitric Acid Solutions: Formation Mechanism of  $\text{NO}_3^\bullet$  Radical. *J. Phys. Chem. A* **2012**, *116*, 7302–7307.
- (11) El Omar, A. K.; Schmidhammer, U.; Balcerzyk, A.; LaVerne, J.; Mostafavi, M. Spur Reactions Observed by Picosecond Pulse Radiolysis in Highly Concentrated Bromide Aqueous Solutions. *J. Phys. Chem. A* **2013**, *117*, 2287–2293.
- (12) Allen, A. O. The Yields of Free H and OH in the Irradiation of Water. *Radiat. Res.* **1954**, *1*, 85–96.
- (13) Barr, N. F.; Schuler, R. H. The Dependence of Radical and Molecular Yields on Linear Energy Transfer in the Radiation Decomposition of 0.8 N Sulfuric Acid Solutions. *J. Phys. Chem.* **1959**, *63*, 808–813.
- (14) Hochanadel, C. J.; Ghormley, J. A.; Sworski, T. J. The Decomposition of Sulfuric Acid by Cobalt  $\gamma$ -Rays. *J. Am. Chem. Soc.* **1955**, *77*, 3215–3215.
- (15) Boyle, J. W. The Decomposition of Aqueous Sulfuric Acid Solutions by Cobalt Gamma Rays: I. Radical and Molecular Product Yields from Ce(IV) Solutions in 0.4 to 18 M Acid. *Radiat. Res.* **1962**, *17*, 427–449.
- (16) Boyle, J. W. The Decomposition of Aqueous Sulfuric Acid Solutions by Cobalt Gamma Rays II. Yields of Solvent Decomposition and Reducing Radicals from Fe(II) Solutions in 0.4 to 18 M Acid. *Radiat. Res.* **1962**, *17*, 450–464.
- (17) Daniels, M.; Lyon, J.; Weiss, J. The Formation of Peroxymonosulphuric Acid and Peroxydisulphuric Acid in Solutions of Sulphuric Acid Irradiated by  $^{60}\text{Co}$  Radiation. *J. Chem. Soc.* **1957**, 4388–4390.
- (18) Bibler, N. E. Radiolysis of 0.4 M Sulfuric Acid Solutions with Fission Fragments from Dissolved Californium-252. Estimated Yields of Radical and Molecular Products that Escape Reactions in Fission Fragment Tracks. *J. Phys. Chem.* **1975**, *79*, 1991–1995.
- (19) Sworski, T. J. Relative Rate Constants for Reaction of OH Radical with Sulfuric Acid, Formic Acid and Cerous ions. *J. Am. Chem. Soc.* **1956**, *78*, 1768–1769.
- (20) Heckel, E. Pulsradiolytische Untersuchung Des Radikal-anions  $\text{SO}_4^-$ . *Bunsen-Ges. Phys. Chem., Ber.* **1966**, *70*, 149–54.
- (21) Lesigne, B.; Ferradini, C.; Pucheault, J. Pulse Radiolysis Study of the Direct Effect on Sulfuric Acid. *J. Phys. Chem.* **1973**, *77*, 2156–2158.
- (22) Jiang, P. Y.; Katsumura, Y.; Nagaishi, R.; Domae, M.; Ishikawa, K.; Ishigure, K.; Yoshida, Y. Pulse Radiolysis Study of Concentrated Sulfuric Acid Solutions. Formation Mechanism, Yield and Reactivity of Sulfate Radicals. *J. Chem. Soc. Faraday. Trans.* **1992**, *88*, 1653–1658.
- (23) Matthews, R. W.; Mahlman, H. A.; Sworski, T. J. Elementary Processes in the Radiolysis of Aqueous Sulfuric Acid Solutions. Determinations of Both  $G_{\text{OH}}$  and  $G_{\text{SO}_4^-}$ . *J. Phys. Chem.* **1972**, *76*, 1265–1272.
- (24) Polevoi, A. P.; Khachaturovtavrizian, E. S.; Ivanov, I. N. Pulse Radiolysis of Concentrated Sulfuric Acid. *Radiat. Phys. Chem.* **1990**, *36*, 99–103.
- (25) Kim, K. J.; Hamill, W. H. Direct and Indirect Effects in Pulse Irradiated Concentrated Aqueous Solutions of Chlorides and Sulfate Ions. *J. Phys. Chem.* **1976**, *80*, 2320–2325.
- (26) Choe, Y. K.; Tsuchida, E.; Ikeshoji, T. First Principles Molecular Dynamics Study on Aqueous Sulfuric Acid Solutions. *J. Chem. Phys.* **2007**, *126*, 154510-1–154510-8.
- (27) Kameda, Y.; Hosoya, K.; Sakamoto, S.; Suzuki, H.; Usuki, T.; Uemura, O. Hydrogen-Bonded Structure in Aqueous Sulfuric Acid Solutions. *J. Mol. Liquids* **1995**, *65/66*, 305–308.
- (28) Tang, Y.; Thorn, R. P.; Mauldin, R. L.; Wine, P. H. Kinetics and Spectroscopy of the  $\text{SO}_4^-$  Radical in Aqueous Solution. *J. Photochem. Photobiol., A* **1988**, *44*, 243–258.
- (29) Hayon, E.; Treinin, A.; Wilf, J. Electronic Spectra, Photochemistry, and Autoxidation Mechanism of the Sulfite–Bisulfite–Pyrosulfite Systems. The  $\text{SO}_2^-$ ,  $\text{SO}_3^-$ ,  $\text{SO}_4^-$ , and  $\text{SO}_5^-$  Radicals. *J. Am. Chem. Soc.* **1972**, *94*, 47–57.
- (30) Ma, J.; Schmidhammer, U.; Pernot, P.; Mostafavi, M. Reactivity of the Strongest Oxidizing Species in Aqueous Solutions: The Short-Lived Radical Cation  $\text{H}_2\text{O}^{\bullet+}$ . *J. Phys. Chem. Lett.* **2014**, *5*, 258–261.
- (31) Belloni, J.; Monard, H.; Gobert, F.; Larbre, J. P.; Demarque, A.; De Waele, V.; Lampre, I.; Marignier, J. L.; Mostafavi, M.; Bourdon, J. C.; et al. ELYSE—A Picosecond Electron Accelerator for Pulse Radiolysis Research. *Nucl. Instrum. Methods Phys. Res., Sect. A* **2005**, *539*, 527–539.
- (32) Schmidhammer, U.; El Omar, A. K.; Balcerzyk, A.; Mostafavi, M. Transient Absorption Induced by a Picosecond Electron Pulse in the Fused Silica Windows of an Optical Cell. *Radiat. Phys. Chem.* **2012**, *81*, 1715–1719.
- (33) Muroya, Y.; Lin, M. Z.; Wu, G. Z.; Iijima, H.; Yoshi, K.; Ueda, T.; Kudo, H.; Katsumura, Y. A Re-evaluation of the Initial Yield of the Hydrated Electron in the Picosecond Time Range. *Radiat. Phys. Chem.* **2005**, *72*, 169–172.
- (34) El Omar, A. K.; Schmidhammer, U.; Jeunesse, P.; Larbre, J.-P.; Lin, M.; Muroya, Y.; Katsumura, Y.; Pernot, P.; Mostafavi, M. Time-dependent Radiolytic Yield of  $\text{OH}^\bullet$  Radical Studied by Picosecond Pulse Radiolysis. *J. Phys. Chem. A* **2011**, *115*, 12212–12216.
- (35) Yang, J. F.; Kondoh, T.; Yoshida, Y. Ultrafast Pulse Radiolysis. *Nucl. Instrum. Methods Phys. Res., Sect. A* **2011**, *629*, 6–10.